

Cite this article as: Rare Metal Materials and Engineering, 2020, 49(5): 1593-1600.

ARTICLE

# Effect of Orientations on Tensile Property of Single Crystal $\gamma$ -TiAl Alloys with Certain Vacancy Concentration

Li Haiyan<sup>1,2</sup>, Kou Peipei<sup>1,2</sup>, Li Longlong<sup>1,2</sup>, Feng Ruicheng<sup>1,2</sup>, Cao Hui<sup>1,2</sup>

<sup>1</sup> School of Mechanical and Electrical Engineering, Lanzhou University of Technology, Lanzhou 730050, China; <sup>2</sup> Key Laboratory of Digital Manufacturing Technology and Application, Ministry of Education, Lanzhou 730050, China

**Abstract:** The tensile behavior of  $\gamma$ -TiAl alloys with vacancy defects has been studied by molecular dynamics (MD) simulation considering different lattice orientations. A succession of simulations were performed to analyze the effect of vacancy and lattice orientation on mechanical properties and micro-defect evolution. The results indicate that the orientation has evident impacts on critical stress with Ti and Al vacancy. The yield stress of the model with Ti vacancy is higher than the model containing Al vacancy along three crystal directions. During the deformation of single crystal  $\gamma$ -TiAl alloys, it is found that the dislocation density has the same changeable trend as the number of stacking faults. In addition, the influence of temperature on yield strength also was discussed. The ultimate stress and elastic modulus decrease nonlinearly with the increasing of temperature. The higher temperature results in the less influence of crystal orientation and vacancy defect on the ultimate stress.

**Key words:** TiAl alloys; crystal orientations; vacancy defect; tensile property; dislocation density

TiAl alloys display attractive properties such as low density, high strength, high stiffness and favorable oxidation resistance<sup>[1]</sup>. Therefore, the  $\gamma$ -TiAl alloys have been regarded as the most promising candidates for replacing the heavy Ni-based alloys in the aerospace industry. But the TiAl alloys also have undergone many difficulties during the application process. This is mainly due to its long-range order, which leads to the room temperature brittleness. In addition, there are a large number of defects inevitably generated in the process of reprocessing, such as vacancies, dislocations and stacking faults, which have great impacts on the mechanical properties of  $\gamma$ -TiAl alloys. L. H. Su<sup>[2]</sup> investigated the deformation mechanism during further annealing of the severe plastic deformed materials by commercial purity aluminum processed by equal channel angular pressing. The results show that vacancy-type defects induced by severe plastic deformation play an important part for the strength of the material, such as hardening by annealing and softening by slight deformation in nanosstructured metals. F. Appel<sup>[3]</sup> measured the deformation samples via TEM to study the role of the vacancies of TiAl

alloys in the hardening process. The effects of Ti and Al vacancies at different concentrations on the mechanical properties of  $\gamma$ -TiAl alloys have been investigated by our team.

The atomic density has great variety under different crystal orientations, which lead to the dislocation encountering different resistance. J. P. Wang<sup>[4]</sup> studied the tensile behavior of single crystal nickel with nano-void by molecular dynamics simulation considering different lattice orientations. The results displayed that the dislocation structure begin to nucleate in the stress concentration region. M. A. Bin<sup>[5]</sup> discussed the effect of the orientation on tensile mechanical properties of single crystal tungsten nano-wire. The results indicated that the crystal orientation has little effect on elastic modulus but great impact on tensile strength, yielding strength and ductility, depending on different atomic surface energies and principal sliding planes. In the present work, the tensile properties of  $\gamma$ -TiAl alloys with certain vacancy defects on different crystal orientations were researched by molecular dynamics methods. The effects of crystal orientations on its mechanical proper-

Received date: May 05, 2019

Foundation item: National Natural Science Foundation of China (51865027, 51665030)

Corresponding author: Li Longlong, Master, School of Mechanical and Electrical Engineering, Lanzhou University of Technology, Lanzhou 730050, P. R. China, E-mail: 1282062745@qq.com

Copyright © 2020, Northwest Institute for Nonferrous Metal Research. Published by Science Press. All rights reserved.

ties and micro-defects evolution were studied to provide theoretical basis for optimal design and wide application of the single crystal  $\gamma$ -TiAl alloys.

## 1 Computation Models and Simulation Methods

Large-scale atomic/molecular massively parallel simulation<sup>[6]</sup> (LAMMPS) was used to simulate the influence of orientation on the tensile properties of single crystal  $\gamma$ -TiAl alloys with certain vacancy concentration. In addition, an embedded-atom method (EAM)<sup>[7]</sup> inter-atomic potential was adopted to describe the tensile properties of the single crystal  $\gamma$ -TiAl alloys. The dislocation extraction algorithm (DXA) and common neighbor analysis (CNA) of the open visualization tool (OVITO)<sup>[8]</sup> were used to observe the micro-defect evolution. The  $\gamma$ -TiAl alloys have a space group of P4/mmm and face-center tetrahedral (FCT) structure with L1<sub>0</sub> structure<sup>[9-11]</sup>, which is shown in Fig.1. The lattice constant in three directions are  $a=0.4001$  nm,  $b=0.4001$  nm and  $c=0.418$  10 nm<sup>[12,13]</sup>.

To investigate the impact of crystal orientation on mechanical properties, perfect single crystal  $\gamma$ -TiAl alloys samples were firstly prepared with the three coordinate axes ( $X$ ,  $Y$  and  $Z$ ) along the ([100], [010] and [001]) directions. The size of the model is 90 nm×30 nm×30 nm, including 322 380 atoms. And then the Atomsk software was adopted to rotate the crystal direction and implant vacancy. The model is shown in Fig.2. The parameters are shown in Table 1. Periodic boundary condition was exerted at the left boundary and uniaxially loaded with a constant strain rate of  $2\times10^8$  s<sup>-1</sup> at right boundary during the tensile process. The system is controlled by rescaling the velocities of atoms. The initial velocity keeps to the Maxwell-Boltzmann distribution. Energy minimization and conjugate gradient method are imposed to balance the system. The system temperature is maintained at 300 K by using the Nose-Hoover thermostat in the NPT ensemble, which was applied to the system during the loading process.

## 2 Results and Discussions

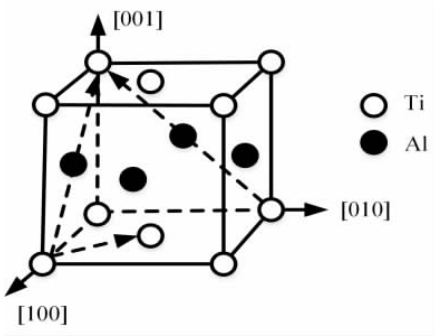


Fig.1 L1<sub>0</sub> structure of  $\gamma$ -TiAl

### 2.1 Stress-strain curves under loading along [100] crystal direction

The effect of vacancy concentrations (0%~3%) on the mechanical properties of  $\gamma$ -TiAl alloys has been studied in previous work. Considering the rapidity of simulation, the vacancy concentration with 1% was adopted in this research. Fig.3 displays the stress-strain curves with vacancy under loading along the [100] crystal orientation. As shown in the Fig.3, the yield stresses of the model containing Ti vacancy and Al vacancy display a great difference in the [100] crystal direction. The ultimate stresses are 8.88 GPa and 8.71 GPa, respectively. They are close to those reported in Ref. [14-16] on the mechanical properties of single crystal  $\gamma$ -TiAl alloys. Dechun Luo<sup>[14]</sup> has researched the propagation of the preset edge crack in the nano single crystal  $\gamma$ -TiAl alloys at different strain rates by the method of molecular dynamics; when the strain rate is  $4\times10^8$  s<sup>-1</sup>, the value of ultimate stress is 5.86 GPa. The results are less than the present paper. The difference of the ultimate stress is mainly dependent on the size of the defect. Therefore, the effect of crack on the strength of the material is stronger than that of the vacancy. H. N. Wu<sup>[15]</sup> has investigated the influence of surface defects with various types and sizes on the tensile deformation and fracture behavior of  $\gamma$ -TiAl under different stain rate and temperature conditions. For a slab defect, the critical stress is 14 GPa at constant strain rate at 300 K. The value is greater than this research. It is because  $\gamma$ -TiAl with surface defects emit the super-dislocation, which plays an important role in material strengthening. Ruicheng Feng<sup>[9]</sup> has similar conclusions about the mechanical properties of single  $\gamma$ -TiAl with different vacancy concentrations.

The yield stress of the model with Ti vacancy is higher than the model containing Al vacancy. The reason for the phenomenon is mainly the difference of diffusion coefficients. It can be expressed by Arrhenius law in Eq.(1)<sup>[16,17]</sup>.

$$D = D_0 \exp\left(-\frac{Q}{kT}\right) \quad (1)$$

Where  $D$  is the diffusion coefficient,  $D_0$  is pre-exponential factor,  $k$  is Boltzmann's factor,  $T$  is temperature.  $Q$  represents vacancy formation energy, whose values are 0.99 and 1.71 eV<sup>[18]</sup> for Al and Ti vacancy, respectively. Therefore, the vacancy diffusion coefficient with Ti vacancy is larger than that with Al vacancy. Meanwhile, the plastic deformation and failure with Al vacancy occur earlier. Vacancies have less effect on the elastic modulus of the  $\gamma$ -TiAl alloys<sup>[9]</sup>. In the elastic stage, the stress increases with the increase of strain. With the occurrence of plastic deformation, brittle fracture finally appears.

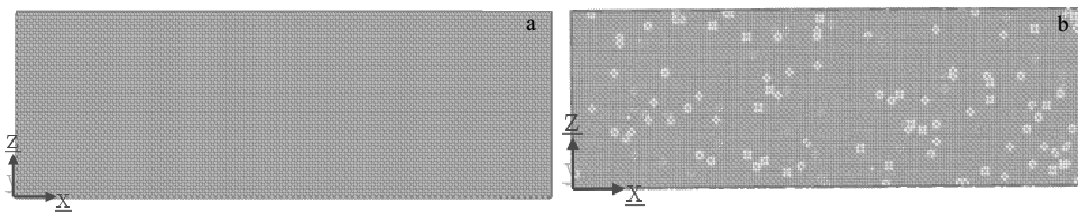


Fig.2 Perfect crystal model (a) and the vacancy concentration with 1% (b): (a) the three axes ( $X$ ,  $Y$  and  $Z$ ) along [100], [010] and [001], (b) the three axes ( $X$ ,  $Y$  and  $Z$ ) along [110],  $[-\bar{1}10]$  and [001]

**Table 1 Parameters for samples under different orientations**

Crystal orientation	$X$	$Y$	$Z$	Number of atoms
[100]	[100]	[010]	[001]	322380
[010]	[110]	$[\bar{1}10]$	[001]	322380
[001]	[111]	$[1\bar{1}2]$	$[\bar{1}10]$	322380

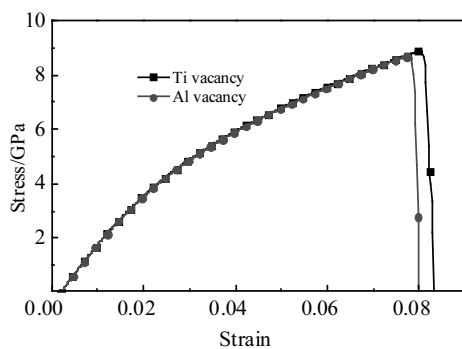


Fig.3 Stress-strain curves under loading along [100] crystal direction

## 2.2 Dislocation nucleation and micro-defect evolution

The effect of crystal direction on dislocation nucleation and material fracture can be clearly illustrated by atomic configuration, which is shown in Fig.4. Fig. 4a indicates that the model with Al vacancy emit the first dislocation at 302 ps. This type of the dislocation is Shockley partial dislocation and the Burgers vector is  $1/6[112]$ . Fig. 4b displays the model with Ti vacancy. It can be seen that the first dislocation emit at 311 ps. The types of the dislocation are Shockley and Frank partial dislocations, and the Burgers vector are  $1/6[112]$  and  $-1/3[111]$ . Supposed the first dislocation emission, it marks the beginning of plastic deformation. Thus, the model with Al vacancy enters the plastic stage earlier, which also shows an earlier fracture failure in the stress-strain curve of Fig.3. The formation of dislocation loops mainly results in the accumulation of vacancies on the close-packed plane, which form a disc. When the disc is large enough, it is energetically favorable for it to collapse and then produce a dislocation loop. The diagram of the dislocation loop forming is shown in Fig.5<sup>[19]</sup>. Fig.5a represents  $\gamma$ -TiAl alloys with a large non-equilibrium concentration of vacancies, Fig.5b represents the vacancies

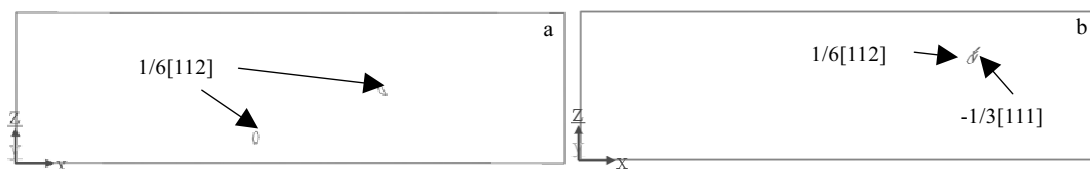


Fig.4 The first dislocation of the models with Al (a) and Ti (b) vacancy are emitted at 302 ps and 311 ps, respectively

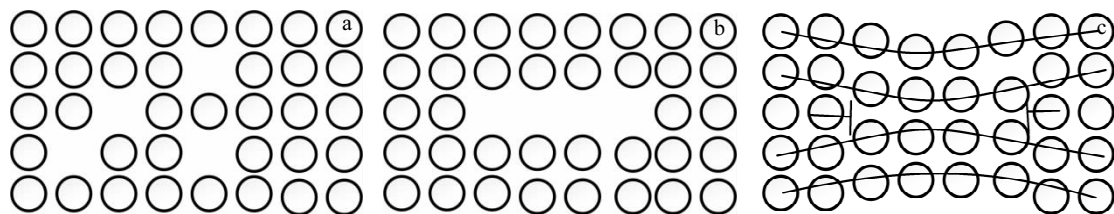


Fig.5 Formulation of a dislocation loop: (a) the  $\gamma$ -TiAl alloys with a large non-equilibrium concentration of vacancies, (b) the vacancies collected on a closed-packed plane, and (c) the disc has collapsed to form an edge dislocation loop

collected on a closed-packed plane, and the disc has collapsed to form an edge dislocation loop, as shown in Fig.5c.

The expansion of the dislocations and stacking faults play an important part on the plastic deformation. For this purpose, the fracture diagrams at different times are shown in Fig.6, where the green exhibit the original fcc structure of  $\gamma$ -TiAl alloys, the blue represents the bcc structure, and the red shows the stacking faults.

It can be observed from Fig.6 that the number of stacking faults increases firstly and then decreases with the increase of loading time. In the early stage of deformation, the number of stacking faults increases due to the aggravation of plastic deformation. With the increase in loading time, voids appear in the material. Stacking faults can end at the position. As a result, the number of stacking faults decreased rapidly at the later stage of deformation. The Lomer-Cottrell dislocation is observed at 309 ps, as shown in Fig.6e. The results are shown in Fig. 7 by DXA analysis. Stacking faults  $S_1$  and  $S_2$  slip in two opposite planes and then meet to form dislocation lock. Correspondingly, the reaction of two partial dislocations forms the stair-rod dislocation. This reaction for [111] and [ $\bar{1}\bar{1}1$ ] planes is shown by  $1/6[\bar{1}2\bar{1}]+1/6[1\bar{1}2]\rightarrow 1/6[011]$ . The stair-rod dislocation serves as an energy barrier to the glide of further dislocation on the two [111] planes. Finally, by comparing the fracture diagram with the dislocation emission, it is found that the dislocation nucleation position is consistent with the final fracture position. One possible reason is that a sta-

ble source of dislocations form in the position of the first dislocation nucleation. The atomic configurations containing Ti vacancy along [100] direction is shown in Fig.8.

In Fig.8, the variation law of the stacking faults is same as the model with Al vacancy. But, compared with Fig.6, the number of Lomer-Cottrell dislocations is more during the deformation process. So, the larger resistance can be provided to the movement of dislocations. It is also why the yield stress of the model containing Ti vacancy is higher than that containing Al vacancy when stretching along [100] crystal orientation. In addition, it is found that the number of dislocations and stacking faults have the same changeable trend through the analysis of CAN and DXA. Finally, the fracture of  $\gamma$ -TiAl alloys has great difference; the model with Ti vacancy lags behind that containing Al vacancy. It can be expressed by Fig.4. Because the time of plastic deformation of the model with Ti vacancy is more lagged. The variations of the dislocation density and the number of stacking faults are shown in Fig.9. Due to the fact that most of the defects of hcp structure are stacking faults, the stacking faults can be represented by the hcp structure. The dislocation length and the number of the stacking faults in two defect models increase firstly and then decrease with the increase of loading time. It is obvious that the number of stacking faults in the model with Ti vacancy is larger than in the one with Al vacancy. And it can also be used to explain the great difference about yield stress along [100] crystal direction. However, the dislocations length of

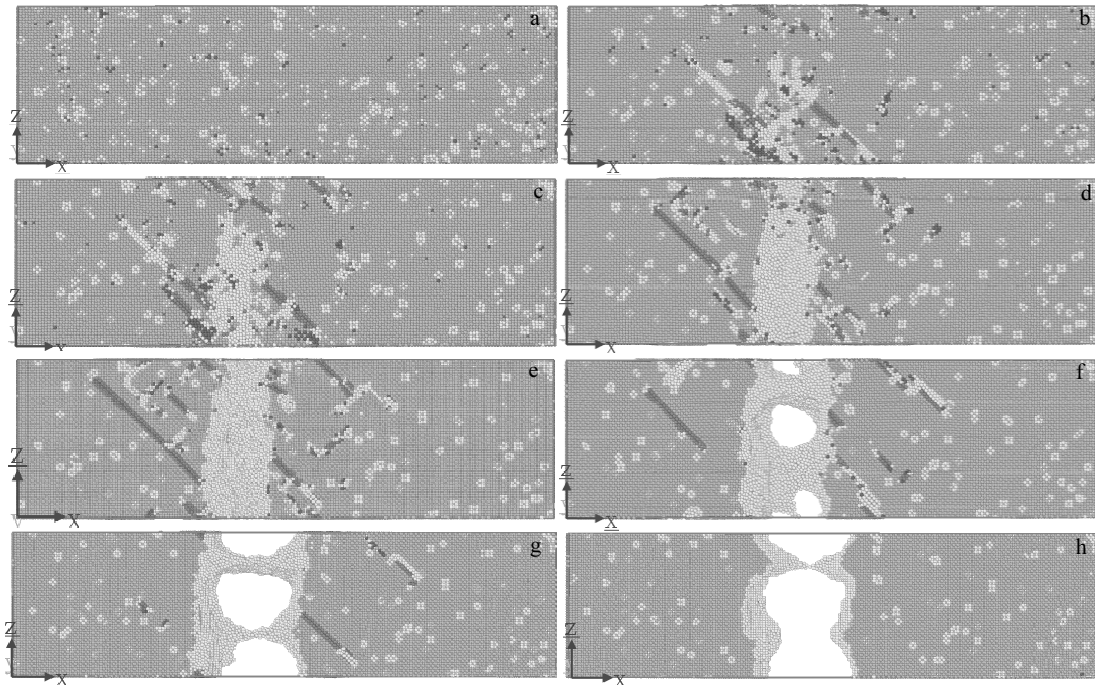


Fig.6 Atomic configurations containing Al vacancy along [100] direction at different time: (a)  $t=302$  ps, (b)  $t=306$  ps, (c)  $t=307$  ps, (d)  $t=308$  ps, (e) 309 ps, (f) 311 ps, (g) 315 ps, and (h) 357 ps

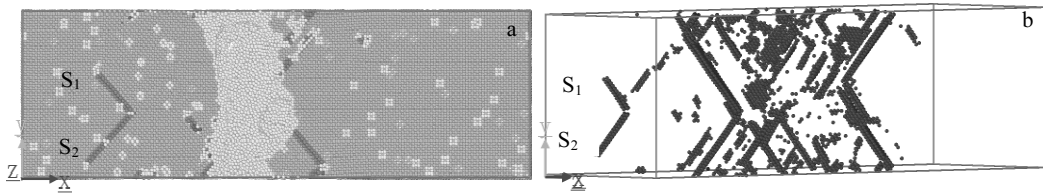


Fig.7 Formulation of a Lomer-Cottrell dislocation in 309 ps

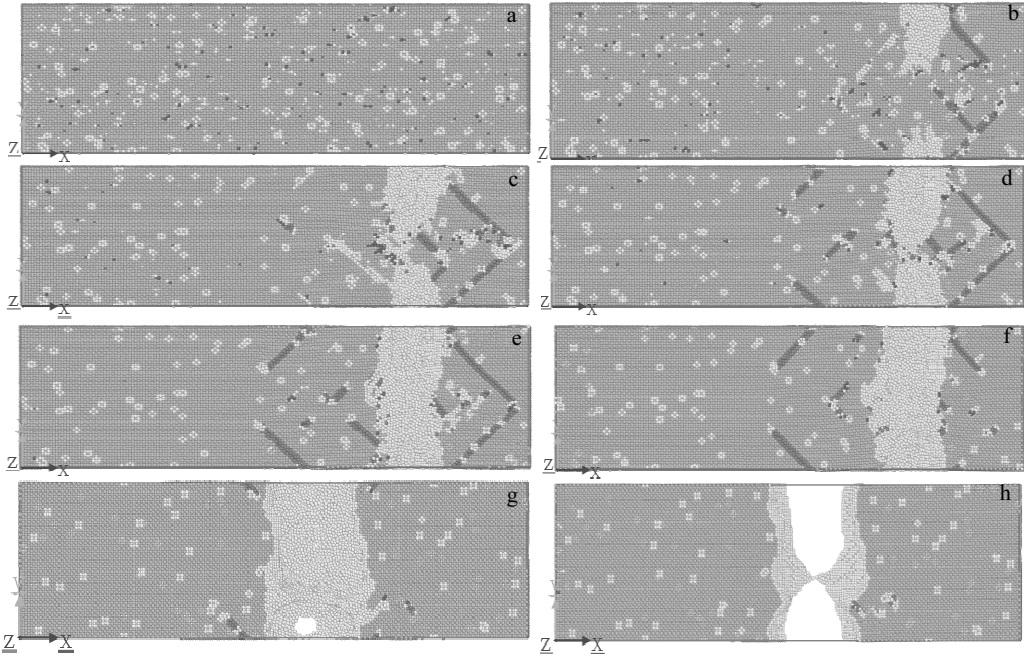


Fig.8 Atomic configurations of containing Ti vacancy for [100] direction at different time: (a) 311 ps, (b) 314 ps, (c) 317 ps, (d) 318 ps, (e) 319 ps, (f) 320 ps, (g) 324 ps, and (h) 397 ps

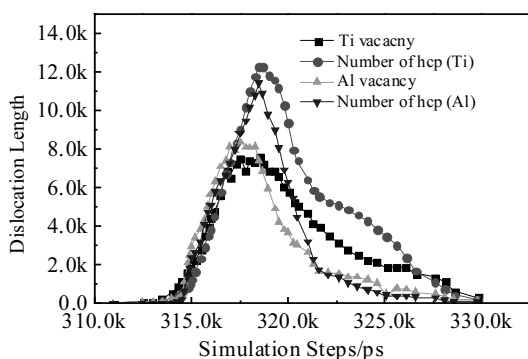


Fig.9 Variation curves of the dislocation length and number of stacking faults

the model with Al vacancy are longer than that of the model with Ti vacancy before 318 ps. Subsequently, the opposite situation occurs. There are two reasons for this phenomenon. Firstly, the plastic deformation of the model with Al va-

cancy occurs earlier, which leads to the longer dislocation length with Al vacancy. Secondly, many dislocation reactions generate the stair-rod dislocations in the model with Ti vacancy. It is the root reason for the increase of the model with Ti vacancy.

### 2.3 Stress-strain curves under loading along [110] and [111]

The stress-strain curves under loading along [110] and [111] directions are shown in Fig.10. Similar to the [100] crystal orientation, the yield stress of the model with Ti vacancy is higher than that of the one with Al vacancy. In the [110] crystal direction, the ultimate stress of two defect models are 9.06 and 8.74 GPa, respectively. However, the ultimate stress of two defect models are 8.94 and 8.68 GPa along the [111] crystal direction. The micro-defects evolution is similar to the [100] crystal direction. The stress of the model with Ti vacancy is relatively high because of the strengthening of dislocations and stacking faults, especially the stair-rod dislocations and Lomer-Cottrell sessile dislocations.

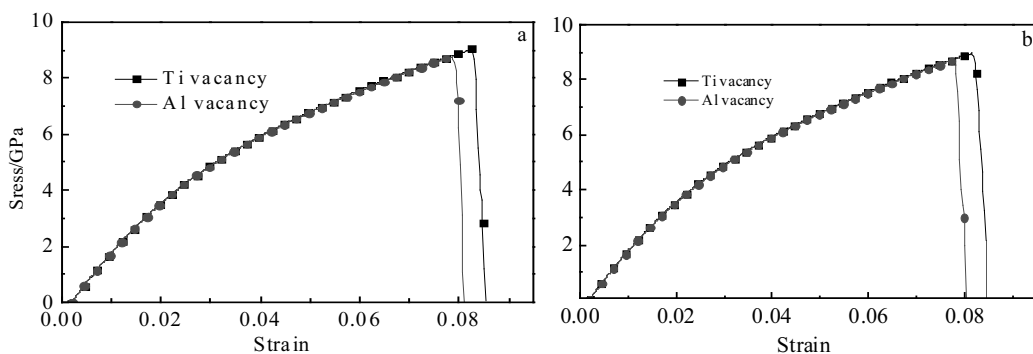


Fig.10 Stress-strain curves under loading along [110] (a) and [111] (b) crystal directions

The above discussions mainly focus on the case where different defect types are in the same crystal orientation. It embodies the role of the defect types and crystal direction. In order to highlight the part of the crystal orientation, a table of mechanical property in the three crystals direction with the defect model was obtained as shown in Table 2. It can be seen from Table 2 that the yield strength of the two defect models reach the maximum value at [110] crystal direction and the minimum at [100] crystal direction. The phenomenon can be attributed to the great difference in the activation of slip system as well as the difference between single and multiple slips. E. M. Bringa<sup>[20]</sup> put forward the following number of slip system with the highest Schmidt factors, as shown in Table 3. In addition, the resolved shear stress is important because it is acknowledged that dislocation motion in fcc single crystal is governed by the critical resolved shear stress via Schmidt's law. Thus, the crystal orientations play an important role on how the Schmidt stress and the stress normal to the slip plane contribute to nucleate dislocations.

Table 4 compares the mechanical properties of  $\gamma$ -TiAl alloys with the results of other scholars. The results of this research are close to the values of experiment. It should be noted that the simulation results are much larger than the experimental values. The result is mainly due to the size effect. When size of the model is small, the strength of material will increase. The conclusion has been proved by many scholars<sup>[4,21]</sup>.

Table 2 Mechanical properties of different crystal orientations (GPa)

Crystal direction/defect type	$[100]_{\text{Ti}}$	$[100]_{\text{Al}}$	$[110]_{\text{Ti}}$	$[110]_{\text{Al}}$	$[111]_{\text{Ti}}$	$[111]_{\text{Al}}$
Ultimate stress	8.88	8.68	9.06	8.74	8.94	8.71
Elastic modulus	178.43	176.67	176.28	175.92	177.25	179.58
Shear modulus	72.53	71.82	71.66	71.51	72.16	72.76

Table 3 Number of slip system with highest Schmidt factors

Crystal direction	Slip system
$[100]$	Eight slip system
$[110]$	Four slip system
$[111]$	Six slip system

Table 4 Comparison of mechanical properties (GPa)

Mechanical properties	F. L. Tang <sup>[22]</sup>	R. C. Feng <sup>[9]</sup>	This research	Experiment <sup>[23]</sup>
Ultimate stress	9.14	9.02	8.88	0.35~0.6
Elastic modulus	143	146	178.4	160~180
Shear modulus	58.13	59.35	72.53	65~73

#### 2.4 Effects of the temperature on the mechanical properties

Because  $\gamma$ -TiAl alloys have good high temperature properties, it has been widely used in various high temperature situations in the past and now. Therefore, it is great meaningful to study the effect of temperature on the mechanical properties of  $\gamma$ -TiAl alloys containing defects. The temperature range for the tensile simulation was chosen from 300 K to 1300 K. The choice of this temperature is mainly based on the characteristics of  $\gamma$ -TiAl alloys. It shows room temperature brittleness at 300 K and the property of brittle-ductile transition occurs between 1000 and 1100 K. In addition, the high temperature creep property is often exhibited when the temperature is beyond 1100 K.

Fig.11 and Fig.12 show the stress-strain curves of single crystal  $\gamma$ -TiAl alloys with a specific vacancy concentration at different temperatures. It can be seen that with the increase of temperature, the elastic modulus and yield stress decrease non-linearly. The decrease of yield stress can be illustrated by Eq.(2)<sup>[24]</sup>.

$$\frac{\tau^*(T)}{\tau^*(0)} = \left(1 - \frac{T}{T_c}\right) \quad (2)$$

where  $\tau^*(0)$  and  $\tau^*(T)$  are the flow stress at 0 K and melting

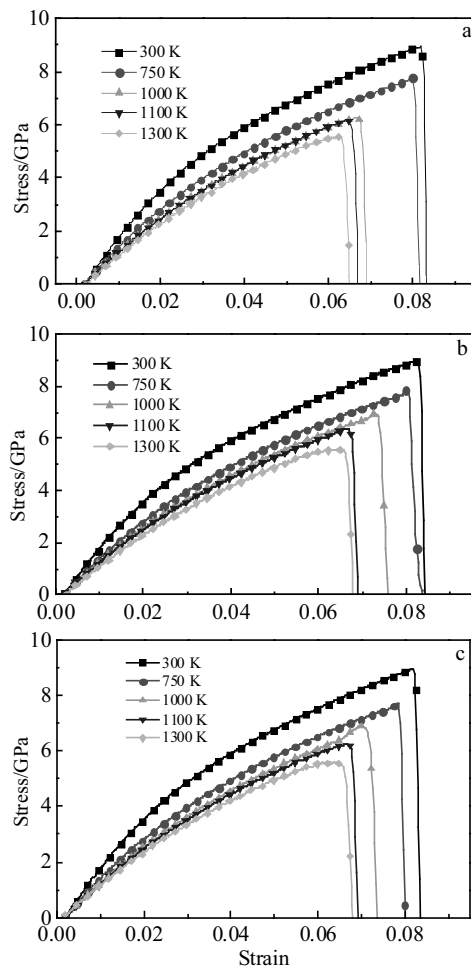


Fig.11 Stress-strain curves of  $\gamma$ -TiAl alloys with Al vacancy at different temperatures: (a), (b) and (c) represent the [100], [110] and [111] crystal directions, respectively

temperature, respectively;  $T$  and  $T_c$  are the temperature and melting temperature, respectively. Hence,  $\tau^*$  decreases from  $\tau^*(0)$  to zero as  $T$  increases from 0 K to  $T_c$ . In fact, the increase of the temperature provides a probability of thermal activation and results in a reduction of flow stress. The decrease of elastic modulus can also be caused by the thermal activation. Tong Liu<sup>[25]</sup> gave the relationship between elastic modulus and temperature at high temperature, as shown in Eq.(3).

$$E = \frac{1}{1 + Ae^{-\Delta G/(kT)}} E_e \quad (3)$$

where  $\Delta G$  is Gibbs free energy;  $A$  is a physical constant related to the micro-defects of materials;  $E$  is elastic modulus;  $E_e$  is the initial value of elastic modulus.

The ultimate stress decreases with the increase of temperature in different crystal orientations, as shown in Fig.13. As the temperature increases, the gap of the ultimate stress in the graph becomes smaller. Thus, the effect of temperature on the mechanical properties of  $\gamma$ -TiAl alloys is greater than that of crystal orientations.

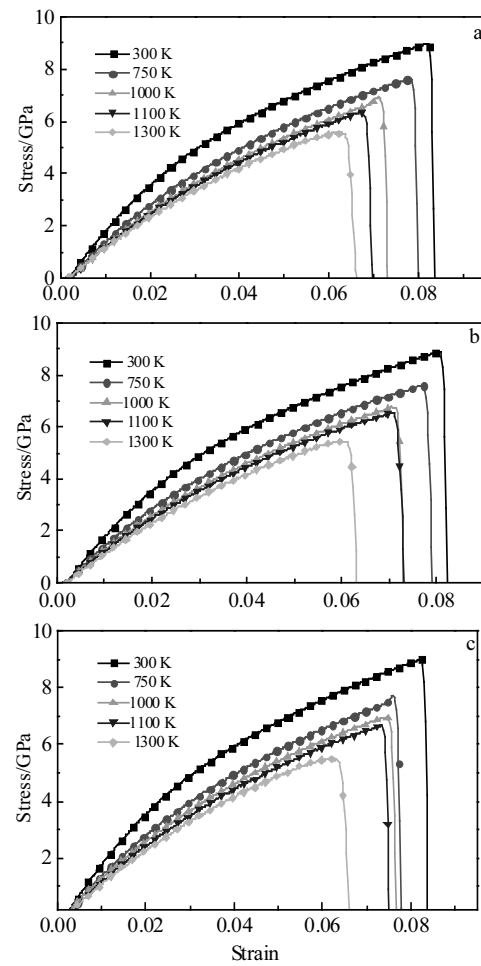


Fig.12 Stress-strain curves of  $\gamma$ -TiAl alloys with Ti vacancy at different temperatures: (a), (b) and (c) display the [100], [110] and [111] crystal directions, respectively

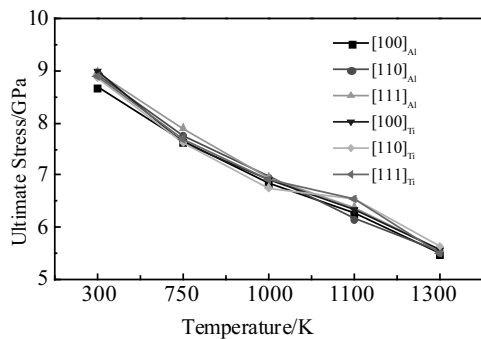


Fig.13 Ultimate stress of  $\gamma$ -TiAl at different temperatures

### 3 Conclusions

- 1) The effect of vacancy concentration on the yield strength of  $\gamma$ -TiAl alloys shows a strong dependence. As the vacancy concentration increases, tensile strength decreases. It is mainly due to the early occurrence of plastic deformation with the increase of vacancy concentration.
- 2) The yield strength of the model with Ti vacancy is

higher than that of the one containing Al vacancy when stretching along [100], [110] and [111]. The phenomenon can be attributed to the difference of diffusion coefficient of Ti and Al vacancy.

3) The results of different orientations simulation show that the stacking faults have a strengthening effect on the yield strength. The critical stresses of the model with Ti vacancy are 8.88, 9.06 and 8.94 GPa along [100], [110] and [111] orientations, respectively. The critical stresses of the model with Al vacancy are 8.71, 8.74 and 8.64 GPa along [100], [110] and [111] orientations, respectively. In the course of simulation, the dislocation density and the number of stacking faults show the same changeable trend.

4) The impact of temperature on the mechanical properties is also considered. The ultimate stress and elastic modulus decrease nonlinearly with the increasing of temperature. It is because the increase of the temperature provides an increase probability of thermal activation and therefore results in a reduction of flow stress and elastic modulus.

## References

- 1 Banumathy S, Neelam N S, Chandravanshi V et al. *Materials Today Proceedings*[J], 2018, 5(2): 5514
- 2 Su L H, Lu C, Tieu A K et al. *Materials Letters*[J], 2011, 65(3): 514
- 3 Appel F, Herrmann D, Fischer F D et al. *International Journal of Plasticity*[J], 2013, 42(1): 83
- 4 Wang J P, Yue Z F, Wen Z X et al. *Computational Materials Science*[J], 2017, 132: 116
- 5 Bin M A, Rao Q H, Yue-Hui H E. *Transactions of Nonferrous Metals Society of China*[J], 2014, 24(9): 2904
- 6 Lehoucq R B, Silling S A, Plimpton S J et al. *Implementation*[J], 2008, 10: 2172
- 7 Srinivasan P, Nicola L, Simone A. *Computational Materials Science*[J], 2017, 134: 145
- 8 Stukowski A. *Modelling Simul Mater Sci Eng*[J], 2010, 18(6): 2154
- 9 Feng Ruicheng, Cao Hui, Li Haiyan et al. *High Temperature Materials & Processes*[J], 2018, 37(2): 113
- 10 Wang Q, Ding H, Zhang H et al. *Materials Characterization*[J], 2018, 137: 133
- 11 Cláudio J DaSilva, José P Rino. *Computational Materials Science*[J], 2012, 62: 1
- 12 Tang F L, Cai H M, Bao H W et al. *Computational Materials Science*[J], 2014, 84: 232
- 13 Feng R, Song W, Li H et al. *Materials*[J], 2018, 11(6): 1025
- 14 Luo Dechun, Zhang Ling, Fu Rong et al. *Rare Metal Materials and Engineering*[J], 2018, 47(3): 853 (in Chinese)
- 15 Wu H N, Xu A S, Wang H et al. *Journal of Materials Science & Technology*[J], 2016, 32: 1033
- 16 Xu Z, Picu C. *Modelling & Simulation in Materials Science & Engineering*[J], 2018, 14(2): 195
- 17 Du Z, Zhang K, Lu Z et al. *Vacuum*[J], 2018, 150: 96
- 18 Wang B, Wang T, Rong Z et al. *Journal of Computer-Aided Materials Design*[J], 1999, 6(2-3): 239
- 19 Hull D, Bacon D J. *Preface-Introduction to Dislocations, Fifth Edition*[M]. Oxford: Butterworth-Heinemann, 2011
- 20 Bringa E M, Traiviratana S, Meyers M A. *Acta Materialia*[J], 2010, 58(13): 4458
- 21 Cheng Ming, Li Ge. *Journal of Shanghai University of Engineering Science*[J], 2012, 26(2): 101 (in Chinese)
- 22 Tang F L, Cai H M, Bao H W et al. *Computational Materials Science*[J], 2014, 84: 232
- 23 Huang Dong, Yang Shaoli, Ma Lan et al. *Iron Steel Vanadium Titanium*[J], 2018, 39(1): 12 (in Chinese)
- 24 Dietze H D. *Zeitschrift für Physik*[J], 1952, 132(1): 107
- 25 Liu Tong, Liu Mingshan. *Materials for Mechanical Engineering*[J], 2014, 38(3): 85

## 晶向对含空位单晶 $\gamma$ -TiAl 合金拉伸性能的影响

李海燕<sup>1,2</sup>, 寇佩佩<sup>1,2</sup>, 李龙龙<sup>1,2</sup>, 冯瑞成<sup>1,2</sup>, 曹卉<sup>1,2</sup>

(1. 兰州理工大学 机电工程学院, 甘肃 兰州 730050)

(2. 数字制造技术与应用省部共建教育部重点实验室, 甘肃 兰州 730050)

**摘要:** 采用分子动力学方法研究了含空位  $\gamma$ -TiAl 合金沿不同晶向下的拉伸性能。通过一系列模拟分析了空位和晶向对力学性能和微观缺陷演化的影响, 结果表明: 晶向对含有 Ti 空位和 Al 空位模型的屈服应力和位错形核机制有明显的影响, 在 3 个晶向上含 Ti 空位模型的屈服应力高于含 Al 空位模型。在单晶  $\gamma$ -TiAl 合金的拉伸变形过程中, 发现位错密度与堆垛层错数目具有相同的变化趋势。此外还讨论了温度对屈服强度的影响, 随着温度的升高, 材料的极限应力非线性下降, 弹性模量明显降低。当温度越高时, 晶向和空位缺陷对  $\gamma$ -TiAl 合金极限应力的影响越小。

**关键词:**  $\gamma$ -TiAl 合金; 晶向; 空位缺陷; 拉伸特性; 位错密度

作者简介: 李海燕, 女, 1979 年生, 硕士, 兰州理工大学机电工程学院, 甘肃 兰州 730050, E-mail: y5217@163.com